Two-stage Kondo effect in side-coupled quantum dots: Renormalized perturbative scaling theory and numerical renormalization group analysis

Chung-Hou Chung,[1,3] Gergely Zarand,[1,2] and Peter Wölfle[1,4]
[1]*Institut für Theorie der Kondensierten Materie, Universität Karlsruhe, 76128 Karlsruhe, Germany*
[2]*Department of Theoretical Physics, Institute of Physics, Budapest University of Technology and Economics, H1111, Budapest, Hungary*
[3]*Electrophysics Department, National Chiao-Tung University, 300, HsinChu, Taiwan, Republic of China*
[4]*Institut für Nanotechnologie, Forschungszentrum Karlsruhe, 76026 Karlsruhe, Germany*
(Received 26 July 2007; published 17 January 2008)

We study numerically and analytically the dynamical (ac) conductance through a two-dot system, where only one of the dots is coupled to the leads but it is also side coupled to the other dot through an antiferromagnetic exchange Ruderman-Kittel-Kasuya-Yoshida (RKKY) interaction. In this case, the RKKY interaction gives rise to a "two-stage Kondo effect" where the two spins are screened by two consecutive Kondo effects. We formulate a renormalized scaling theory that captures remarkably well the crossover from the strongly conductive correlated regime to the low temperature, low conductance state. Our analytical formulas agree well with our numerical renormalization group results. The frequency-dependent current noise spectrum is also discussed.

DOI: 10.1103/PhysRevB.77.035120 PACS number(s): 75.20.Hr, 74.72.−h

INTRODUCTION

The Kondo effect[1] in semiconductor quantum dots has attracted significant theoretical and experimental interest in recent years.[2–4] In a dot that is only weakly coupled to leads, charge fluctuations are typically suppressed due to Coulomb blockade.[5] However, if the dot has an odd number of electrons, then the spin of this electron interacts antiferromagnetically with the spin of the conduction electrons in the leads, and at low temperatures, it is screened through a Kondo effect. The formation of this Kondo state typically leads to an enhancement of the conductance at low bias voltages.

Recently, in the quest for designing multiple quantum dot systems with tunable spin control, which can be used in spintronics and quantum information processing, double quantum dots have become the focus of interest.[6,7] In these systems, when both dots are tuned to the single spin regime, an effective spin-spin interaction known as the Ruderman-Kittel-Kasuya-Yoshida[8] (RKKY) interaction is mediated between the two dots by the conduction electrons.[6] This RKKY coupling competes with the Kondo effect in these systems. In the case where the two dots are coupled to two separate electrodes, an antiferromagnetic RKKY interaction leads to a crossover between the Kondo and RKKY regimes:[6,9–12] A sufficiently strong antiferromagnetic RKKY coupling will lock the spins of the two dots into a singlet and thereby suppress the Kondo effect, while the Kondo effect persists for weak RKKY interactions. This picture is slightly modified under nonequilibrium conditions. Then, even for strong RKKY interaction, the Kondo effect is partially restored by the finite bias voltage allowing for triplet excitations.[13] Part of the rich physics has been studied previously in the framework of two impurity Kondo[14] and Anderson impurity[15] models, and the singlet-triplet crossover has also been recently studied experimentally by Craig *et al.*,[6] who observed the Kondo resonance for weak RKKY couplings and a splitting of the Kondo resonance for large RKKY interactions. Significant theoretical and experimental effort has been devoted to the Kondo-RKKY transition in these double quantum dot systems, and related multiorbital systems with two Kondo-screening channels have also been studied extensively in recent years by different theoretical approaches.[16]

Rather than studying the usual singlet-triplet transition itself, in the present paper, we shall focus on an even simpler but equally interesting arrangement, where only one of the dots is coupled to external leads, but the two dots are still side coupled to each other (see Fig. 1). Unlike the usual four lead setup, where the crossover between a RKKY and Kondo regimes is governed by a quantum critical point corresponding to a finite value of the RKKY coupling J,[11,12] in this side-coupled system, the side-coupled spin is always screened for any positive J, and a Kosterlitz-Thouless-type quantum phase transition and a two-stage Kondo effect occur.[17,18] We remark that this transition is essentially the two-dot analog of the singlet-triplet quantum phase transition found in single dot devices, when the two dot levels are coupled to a single conduction electron mode in the leads.[19,20]

Although many interesting results have been obtained recently for this side-coupled system,[17,18] there is still a lack of a detailed analytical and numerical understanding of the two-stage Kondo screening processes in the vicinity of the quantum phase transition. The main goal of the present work is to have some more detailed theoretical control and understand-

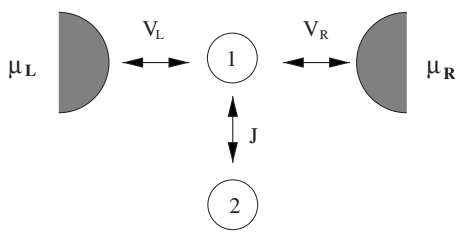

FIG. 1. Sketch of the two side-coupled quantum dots. Electrons tunnel from only one of them to the leads and they interact through an effective exchange interaction J.

ing of the transport properties of this transition. We shall reach this goal by combining numerical renormalization group[21] and renormalized perturbative scaling approaches. As we shall see, the latter relatively simple analytical framework is able to account for the numerical results over a wide range of energy scales, and together with Fermi-liquid theory, it provides a reliable theoretical framework to understand the low energy crossover.

We mostly focus on the T matrix but also present results on the linear ac conductance and the equilibrium current fluctuations. Both of these quantities can be observed experimentally and show features characteristic of the two-stage Kondo effect.

MODEL

For the numerical calculations, we shall describe the two side-coupled dots in Fig. 1 by an Anderson-like model. The two isolated dots are described by the Hamiltonian

$$H_{DD} = \sum_{i=1,2} \frac{U_i}{2}(N_i - n_{gi})^2 + J\mathbf{S}_1\mathbf{S}_2, \tag{1}$$

where $i=1,2$ labels the two dots, $N_i=\Sigma_\sigma d_{i\sigma}^\dagger d_{i\sigma}$ is the number of electrons occupying dot i, and $\mathbf{S}_i=(1/2)\Sigma_{\sigma\sigma'} d_{i\sigma}^\dagger \sigma_{\sigma\sigma'} d_{i\sigma'}$ is their spin. Each dot is subject to a *charging energy*, $U_1 \approx U_2 = U = E_C$, and the two dots are coupled by an exchange coupling, which is assumed to be antiferromagnetic, $J>0$. The n_{gi} in Eq. (1) denote dimensionless gate voltages that set the occupation numbers, $\langle N_i\rangle$. In the rest of the paper, we restrict ourselves to the case of particle-hole symmetry, $n_{g1}=n_{g2}=1$. However, this assumption is expected to be unimportant as long as $n_{g1}\approx n_{g2}\approx 1$.

The coupling of dot 1 to the leads is modeled by the usual tunneling Hamiltonian

$$H_t = \sum_{\alpha=L,R}\sum_{\epsilon,\sigma}(V_\alpha c_{\alpha\epsilon\sigma}^\dagger d_{1,\sigma} + \text{H.c.}). \tag{2}$$

Here, V_L and V_R denote the tunneling amplitudes to the left and right leads, respectively, and $c_{\alpha\epsilon\sigma}^\dagger$ creates an electron in lead $\alpha=L,R$ with spin σ and energy ϵ. This tunnel coupling leads to a broadening of the level on dot 1, the width of which is given by $\Gamma=\Gamma_L+\Gamma_R=2\pi(V_L^2\varrho_L+V_R^2\varrho_R)$, with $\varrho_{L/R}$ the density of states in the leads.

ac CONDUCTANCE AND NOISE

Our main goal is to determine ac transport properties in the linear response regime and see how the two-stage effect appears in these quantities. Fortunately, since there is no charge transfer between the two dots, the derivation of Ref. 22 carries over to our case, and the real part of the optical conductance is simply given by

$$G'(\omega) = \frac{G_0}{4\omega}\sum_\sigma \int d\omega'[f(\omega'-\omega) - f(\omega'+\omega)]T_\sigma(\omega'), \tag{3}$$

where $T(\omega)$ is the "transmission probability" at energy ω, $f(\omega)$ is the Fermi function, and

$$G_0 = \frac{2e^2}{h}\frac{4\Gamma_L\Gamma_R}{(\Gamma_L+\Gamma_R)^2} \tag{4}$$

denotes the maximum conductance through the dot. The transmission coefficient $T_\sigma(\omega)$ appearing in Eq. (3) can be expressed as

$$T_\sigma(\omega) = -\Gamma\ \text{Im}\ G_{11\sigma}(\omega), \tag{5}$$

where we have introduced the retarded Green's function on dot 1: $G_{11\sigma}(t)=-i\theta(t)\langle\{d_{1\sigma}(t), d_{1\sigma}^\dagger\}\rangle$. The transmission coefficient above is essentially the same as the single particle matrix element of the on-shell many-body T matrix.[23] We remark that Eq. (3) neglects displacement currents.[24] This approximation is justified in the Coulomb blockade regime,[25] i.e., for large charging energies and relatively large conductances that satisfy $G(\omega)/G_0 \gg \omega/E_C$.

The Green's function above can be computed accurately using numerical renormalization group methods,[21] but as we shall see, substantial analytical progress can be made by a special version of renormalized perturbation theory.[1] Although Eq. (5) is valid at any temperature, in the following, we shall focus our attention to the high-frequency regime, $\omega \gg T$, and set the temperature to zero, $T=0$.

The noise spectrum of the device is also of experimental relevance. This is defined as

$$C(\omega) = \int_{-\infty}^{\infty} dt e^{i\omega t}[\langle I(0)I(t)\rangle - \langle I\rangle^2]. \tag{6}$$

At equilibrium, this is simply related to the linear conductance $G'(\omega)$ by the fluctuation-dissipation theorem,[22]

$$C(\omega) = \frac{2\hbar\omega}{\exp(\hbar\omega/kT)-1}G'(\omega). \tag{7}$$

This formula simplifies further at $T=0$ temperature to $C(\omega)=2\hbar|\omega|G'(\omega)\theta(-\omega)$. Clearly, to determine the equilibrium noise spectrum of the device and its ac conductance, only the Green's function of the first dot needs to be determined.

RENORMALIZED PERTURBATIVE SCALING

Before presenting our numerical results, let us reach some analytical understanding of the physics of the side-coupled dot in the limit $J\to 0$. In this regime, "two-stage Kondo screening" takes place:[17] In the first stage, the spin of dot 1 gets screened below the Kondo temperature $T_K \approx De^{-\pi U/\Gamma}$, where the high energy cut-off D denotes the effective half bandwidth of the conduction electrons.[26] Clearly, for the Kondo effect to take place, $J \ll T_K$ is required; otherwise, the two spins are locked together to a singlet before the Kondo effect can take place. Then, below the Kondo scale T_K, the electron on the first dot is dissolved in the conduction electron sea of the leads and presents an effective fermionic bath for the electron on the second dot. Since the coupling between the two dots is antiferromagnetic, another Kondo effect shall take place at a much smaller energy scale $T^\star$, where the spin of the second dot is also screened. Our aim is to understand the formation of this second Kondo singlet in detail.

We first observe that in the regime of interest, $\omega \ll T_K$, the Matsubara Green's function of dot 1 can be approximated by the resonant level expression[1]

$$G_{d1}^0(i\omega_n) = \frac{z}{i\omega_n + i\tilde{T}_K \,\mathrm{sgn}(\omega_n)}, \tag{8}$$

where $z = c\frac{T_K}{\Gamma}$ denotes the quasiparticle weight at the Fermi energy, and $\tilde{T}_K = z\Gamma = cT_K$ is an energy of the order of the Kondo temperature T_K. The precise value of the universal constant c relating T_K and $\tilde{T}_K$ depends on the definition of T_K. Throughout this paper, we shall define T_K as the half-width of the transmission $T(\omega)$. Then, from fitting the numerical renormalization group (NRG) data, we get $c \approx 0.5$. Note that the Lorentzian representing the Kondo resonance has a very small spectral weight, $z \ll 1$, and most of the spectral weight goes to the Hubbard peaks.

Fermi-liquid theory and the basic principles of renormalization group also imply that the exchange interaction between the dot spins is renormalized by the same z factor, i.e., in the regime $\omega \ll T_K$, the effective RKKY interaction reads

$$H_{\mathrm{RKKY}} \to \frac{\tilde{J}}{z}\mathbf{S}_1\mathbf{S}_2. \tag{9}$$

In a first approximation, one would think that $\tilde{J}=J$; however, the fact that $\mathrm{Im}\, G_{d1}$ has a large logarithmic tail above T_K leads to a slight renormalization of this relation. From a fitting of the numerical data shown later, we obtain the approximate relation $\tilde{J} \approx 1.1J$.

We are now in the position to develop a perturbative scaling theory in the small coupling, $\tilde{J}$. To do this, we used Abrikosov's pseudofermion representation to compute the second order self-energy and vertex corrections, shown in Fig. 2. The dimensionless vertex function is given by the following expression:

$$\gamma(\omega) \equiv \varrho(\omega)\Gamma(\omega) = \hat{\varrho}(\omega)\tilde{J} + [\hat{\varrho}(\omega)\tilde{J}]^2 \log\left(\frac{\tilde{T}_K}{-\omega}\right)\cdots, \tag{10}$$

where $\tilde{T}_K = cT_K$ is the effective width of the Kondo resonance, ω is the energy of the incoming electron, and $\hat{\varrho}(\omega)$ denotes the rescaled effective density of states of dot 1, serving as a many-body reservoir for dot 2,

$$\hat{\varrho}(\omega) \equiv \frac{\varrho(\omega)}{z} = \frac{\tilde{T}_K}{\pi(\omega^2 + \tilde{T}_K^2)}. \tag{11}$$

Equation (10) is only of logarithmic accuracy, irrelevant terms of order $\omega/\tilde{T}_K$ have been neglected.

The Kondo temperature $T_K \sim \tilde{T}_K$ appears in Eq. (10) as a high energy cutoff. We can therefore perform a scaling transformation by reducing this cutoff, $\tilde{T}_K \to \tilde{T}'_K$, and requiring the invariance of the vertex function for frequencies $\omega < \tilde{T}_K$ at the same time. This transformation sums up all leading logarithmic diagrams and leads to the following scaling equation:

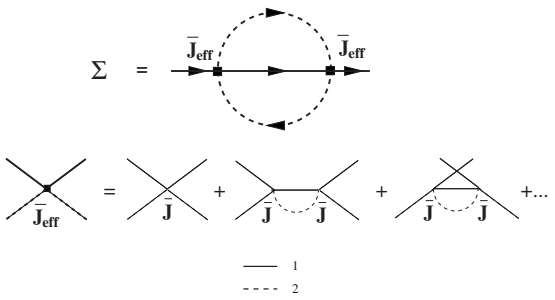

FIG. 2. Top: leading logarithmic contribution to the self-energy of the first dot's Green's function. Solid lines represents the propagator G_{d1}^0 of quantum dot 1, given by Eq. (8), while dashed lines denote the pseudofermion propagator associated with the side-coupled dot's spin S_2. Full squares stand for the full leading logarithmic vertex function, given in the lower part of the figure. Crossings of dashed and continuous lines correspond to an interaction through the renormalized RKKY interaction, $J_{\mathrm{eff}} = \tilde{J}/z$, given by Eq. (9).

$$\frac{d[\hat{\varrho}(\omega)\tilde{J}]}{dl} = [\hat{\varrho}(\omega)\tilde{J}]^2, \tag{12}$$

with the scaling variable defined as $l \equiv \log(\tilde{T}_K/\tilde{T}'_K)$. Integrating this differential equation up to $l \equiv \log(\tilde{T}_K/\omega)$, one obtains the dimensionless vertex function in the leading logarithmic approximation:

$$\gamma(\omega, \tilde{T}_K) = \frac{\hat{\varrho}(\omega)\tilde{J}}{1 + \hat{\varrho}(\omega)\tilde{J}\log(-\omega/\tilde{T}_K)}. \tag{13}$$

This equation can be rewritten with a little algebra as

$$\gamma(\omega, \tilde{T}_K) = \frac{1}{\frac{\omega^2}{\tilde{T}_K^2}\log\frac{\tilde{T}_K}{T^*} + \log\frac{-\omega}{T^*}}, \tag{14}$$

with the second scale T^* defined as

$$T^* = \tilde{T}_K \exp(-\pi\tilde{T}_K/\tilde{J}). \tag{15}$$

This scale also appears in the slave boson approach of Ref. 17. However, while the slave boson approach describes correctly the Fermi-liquid regimes, $\omega \ll T^*$ and $T_K/\ln(T_K/T^*) \ll \omega \ll T_K$, it cannot account for the logarithmic corrections dominating the rather extended crossover regime, $T^* < \omega < T_K/\ln(T_K/T^*)$, that is of our main interest here.

Clearly, the dimensionless vertex diverges at an energy $\omega \approx T^*$, implying that the effective RKKY interaction becomes dominant below this scale and diverges in the limit $\omega \to 0$.[21] In other words, below T^*, a singlet is formed from the two dot spins, and the scale T^* can thus be viewed as the effective singlet-triplet binding energy. Note that the spin singlet is always the ground state for any arbitrary RKKY coupling $J > 0$.

The point $\tilde{J}=0$ is special: It separates the ferromagnetic phase ($J<0$) from the antiferromagnetic phase discussed so far ($J>0$). While in the antiferromagnetic phase the two dot

spins are locked into a singlet, in the ferromagnetic phase, the spins of the dots are bound to a triplet, which is then partially screened by the lead electrons, and correspondingly, the ground state is a doublet for $J<0$. Thus, for $J<0$, the side-coupled system has a residual entropy. At the critical point, $J=0$, the scale T^* diverges exponentially, corresponding to a Kosterlitz-Thouless phase transition between these two states.[17,18]

The second order self-energy correction to the retarded Green's function G_{d1}^0 simply gives the expression

$$\Sigma(\omega) = S(S+1)\frac{\tilde{J}^2}{4z}\frac{1}{\omega + i\tilde{T}_K}, \tag{16}$$

where $S=1/2$. Note that this correction scales as $\sim J^2/(T_K z)$ and, although it looks to be very large at first sight, it is actually small compared to $(G_{d1}^0)^{-1} \sim T_K/z$ as long as $J \ll T_K$. In the leading approximation, this self-energy results in the following Green's function:

$$\Gamma G_d^{(2)}(\omega) = \frac{\tilde{T}_K}{\omega + i\tilde{T}_K - \dfrac{\tilde{J}^2 S(S+1)}{4}\dfrac{1}{\omega + i\tilde{T}_K}}. \tag{17}$$

Summing up the leading logarithmic corrections to the self-energy simply amounts to replacing $\tilde{J}$ in Eq. (17) by $\gamma(\omega)/\hat{\varrho}(\omega)$ and thereby results in the following transmission coefficient:

$$T_\sigma(\omega) = -\,\mathrm{Im}\left\{\frac{\tilde{T}_K^3}{\omega\left[\tilde{T}_K^2 - \frac{1}{4}S(S+1)\pi^2(\omega^2+\tilde{T}_K^2)\gamma^2(\omega)\right] + i\tilde{T}_K\left[\tilde{T}_K^2 + \frac{1}{4}S(S+1)\pi^2(\omega^2+\tilde{T}_K^2)\gamma^2(\omega)\right]}\right\}. \tag{18}$$

The logarithmic corrections hidden in γ result in the formation of a dip in the spectral density of dot 1, corresponding to a *suppression* of the transmission coefficients at energies $\omega \sim T^* \ll T_K$. This dip in $T_\sigma(\omega)$ also implies the appearance of a dip in the ac conductance discussed later and is a clear signature of the formation of a singlet ground state. Physically, it is a consequence of the fact that electrons promoted from one side of the device to the other must first break up the singlet of energy T^* formed by the two dot spins. Clearly, electrons of energy $\omega < T^*$ are not energetic enough to break up this singlet and therefore their transport is suppressed.

The logarithmic approximation breaks down below $\omega \sim T^*$. There a Fermi liquid is formed and $T_\sigma(\omega)$ scales as

$$T_\sigma(\omega) \approx a + b\frac{\omega^2}{(T^*)^2} \quad (\omega \ll T^*). \tag{19}$$

The constant a vanishes for electron-hole symmetry and remains typically small unless electron-hole symmetry is dramatically broken, while the coefficient b is a number of the order of unity.

COMPARISON WITH NUMERICAL RENORMALIZATION GROUP

The transport properties of the side-coupled quantum dot system can also be studied numerically by numerical renormalization group (NRG) methods. The transmission coefficient $T(\omega)$ through dot 1 obtained from NRG at different RKKY couplings J is plotted in Fig. 3. In all figures, we compensated for a 6% loss of the spectral weight. The large resonance is a manifestation of the Kondo effect displayed by the first dot, and the sharp dips in the transmission at $\omega \approx 0$ are due to the formation of the singlet state below the energy T^*.

The numerically obtained transmission coefficients are compared to the analytical formula [Eq. (18)] in Fig. 4. The perturbative expression agrees well with the numerical results over a wide range of energy scales between T^* and T_K. It is interesting to observe the deviations *above* T_K, where the simple Lorentzian approximation we made for $G_d^{(0)}$ fails to account for the fact that the resonance on dot 1 is also a Kondo resonance. This Lorentzian approximation thus completely neglects the large logarithmic tails for $\omega > T_K$. In the

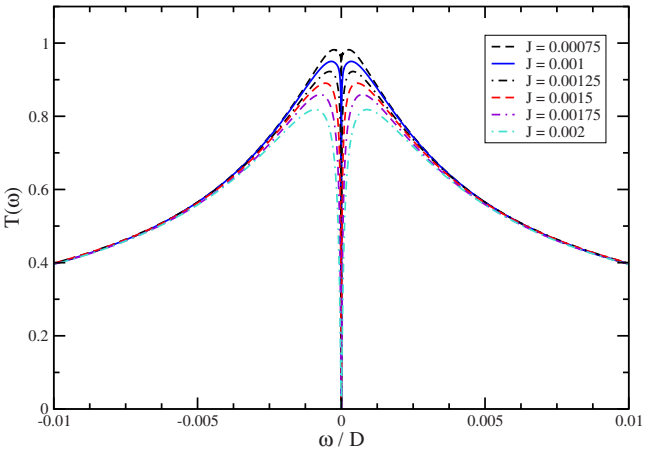

FIG. 3. (Color online) Transmission coefficient through dot 1 at zero temperature for different RKKY couplings J. The energy unit is the half bandwidth, $D=1$. The Anderson model's parameters were $U=1$, $\epsilon_{d1}=\epsilon_{d2}=-0.5$, and $\Gamma_{1L}=\Gamma_{1R}=0.1$, resulting in a Kondo temperature of $T_K \approx 0.0055$. We used a discretization parameter $\Lambda=2$.

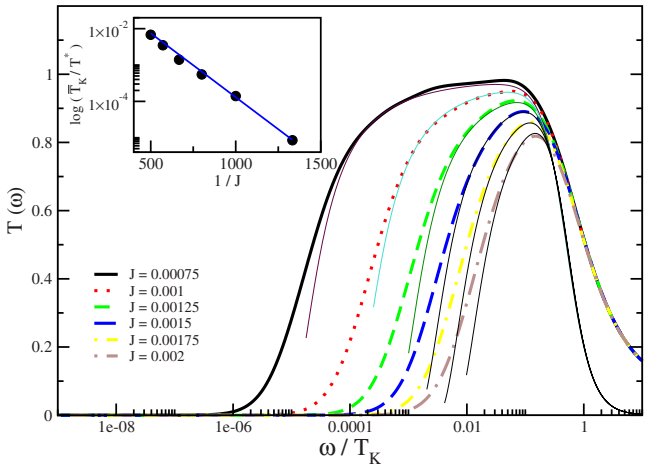

FIG. 4. (Color online) Fit of the numerically obtained transmission coefficient $T(\omega)$ by the perturbative expression [Eq. (18)] for various values of $\tilde{J}$. For all fits, we used $\tilde{T}_K=0.5T_K=0.003$. The inset shows the scale T^* extracted from the fit as a function of $1/J$.

inset, we also show the scale T^* as extracted from our fits as a function of $1/J$. The extracted scales compare very well with the analytical expression, Eq. (15), indicated by the solid line.

The two-stage Kondo effect and the K-T transition can also be observed in the ac conductance of the two-dot device or the noise spectrum. Such measurements have been indeed done in recent experiments of high-frequency current fluctuations,[27] though the linear ac conductance measurements in the relevant frequency regime are very difficult due to background currents from the capacitors.[28] According to Eq. (3), the real part of the conductance through the device can be computed from the transmission coefficient through a simple integration. The resulting curves are displayed in Fig. 5.

It is interesting to remark that the low energy crossover of the transmission coefficient and the conductance is described by *universal crossover functions* for $\omega, T^* \ll T_K$.[29] The conductance, e.g., is approximately given by

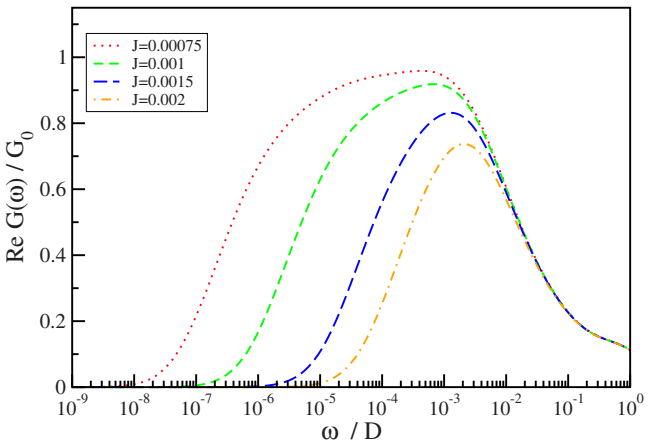

FIG. 5. (Color online) ac conductance normalized by G_0 for the same parameters as in Fig. 3.

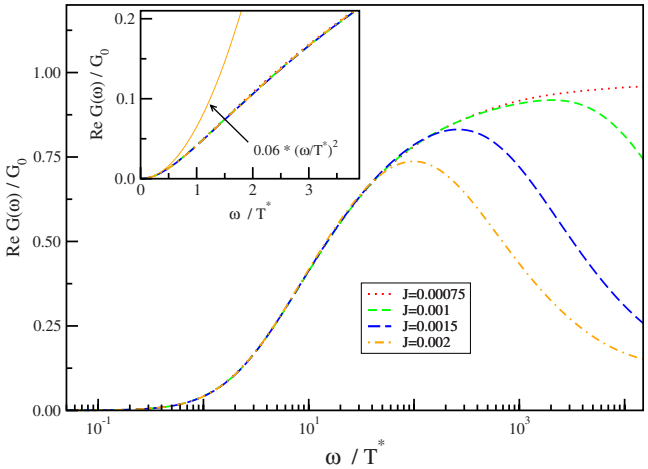

FIG. 6. (Color online) $G'(\omega)$ as a function of ω/T^* for various values of J. Below the Kondo scale, all curves collapse to a universal curve. Inset: small frequency part of this universal curve on a linear scale. We also show the quadratic behavior characteristic of electron-hole symmetry, determined from a log-log fit of the curves.

$$G'(\omega) \approx G_0 g(\omega/T^*) \tag{20}$$

in this regime. Here, the scaling function g depends somewhat on electron-hole symmetry breaking, but in case of electron-hole symmetry, it is completely universal. Then, for very small frequencies, it scales to zero as $g(\omega) \approx 0.06(\omega/T^*)^2$, while at high energies, it approaches 1 logarithmically, $g(\omega/T^*) \approx 1-\alpha/\log^2(\omega/T^*)$. This universal crossover function can be extracted from the NRG results and is displayed in Fig. 6. The transmission coefficient $T_\sigma(\omega)$ displays similar universal scaling properties.

Finally, let us discuss the current noise at zero temperature, plotted in Fig. 7. At $T=0$ temperature, $C(\omega)$ has only weight for $\omega<0$. For $T^*<-\omega<T_K$, we have $C(\omega) \propto |\omega|$ cor-

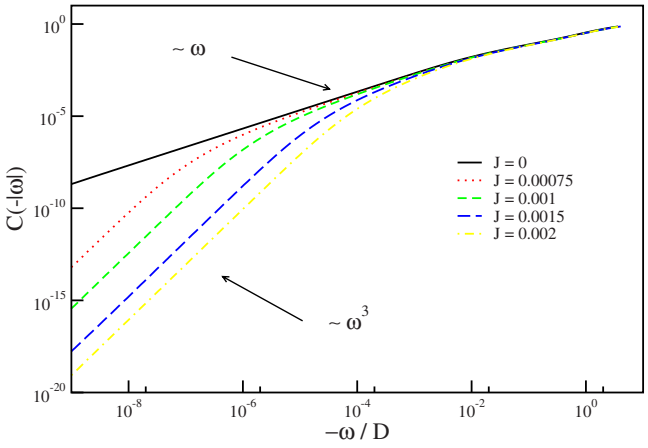

FIG. 7. (Color online) Equilibrium current noise $C(\omega)$ in case of electron-hole symmetry for $\omega<0$. $C(\omega)$ exhibits linear dependence on ω for $T^*<|\omega|<T_K$ that crosses over to a cubic behavior below T^*. Note that $C(\omega)=0$ for $\omega>0$. The parameters are the same as in Fig. 3.

responding to the Fermi-liquid property of a perfectly transmitting quantum dot.[22] However, for $-\omega < T^*$, this behavior crosses over to a power law scaling, where in the case of electron-hole symmetry one has $C(\omega) \propto |\omega|^3/(T^*)^2$. This behavior is somewhat modified once electron-hole symmetry is broken. Then, the conductance remains finite even in the $\omega \to 0$ limit, and correspondingly, another crossover may take place from the $C(\omega) \propto |\omega|^3$ regime to a linear regime, $C(\omega) \propto |\omega|$, at some energy $T^{**} \ll T^*$. Note that the axis of the logarithmic plot in Fig. 7 has not been rescaled, in contrast to Fig. 6. However, the low-frequency part of $C(\omega)/T^*$ would also exhibit a universal crossover as a function of ω/T^*, similar to $G(\omega)$.

CONCLUSIONS

We provided a complete analytical and numerical analysis of the ac transport properties and the two-stage Kondo screening in side-coupled quantum dots. Our analytical results were based on renormalized perturbation and scaling theory, and they agree well with the NRG result over a wide frequency range. We also determined the linear ac conductance and the equilibrium current noise which can both be measured experimentally and reflect the two-stage Kondo effect and the *K*-*T* transition. We also computed the universal crossover functions that describe the emergence of the triplet state at the energy T^*.

ACKNOWLEDGMENTS

This work has been supported by the DFG-Center for Functional Nanostructures and by the Virtual Institute for Research on Quantum Phase Transitions at the University of Karlsruhe. C.-H.C acknowledges the support from the NSC, the NCTS, and the MOE ATU Program of Taiwan, ROC. G.Z. has been supported by the Humboldt Foundation and by Hungarian grants, OTKA No. NF061726, and T046303. He also acknowledges the hospitality of the CAS, Norway, where part of this research has been done.

[1] A. C. Hewson, *The Kondo Problem to Heavy Fermions* (Cambridge University Press, Cambridge, England, 1997).
[2] L. Kouwenhoven and L. Glazman, Phys. World **14**, 33 (2001).
[3] D. Goldhaber-Gordon, H. Shtrikman, D. Mahalu, D. Abusch-Magder, U. Meirav, and M. A. Kastner, Nature (London) **391**, 156 (1998); S. M. Cronenwett, T. H. Oosterkamp, and L. P. Kouwenhoven, Science **281**, 540 (1998); F. Simmel, R. H. Blick, J. P. Kotthaus, W. Wegscheider, and M. Bichler, Phys. Rev. Lett. **83**, 804 (1999); J. Schmid, J. Weis, K. Eberl, and K. v. Klitzing, *ibid.* **84**, 5824 (2000); W. G. van der Wiel *et al.*, Science **289**, 2105 (2000).
[4] L. I. Glazman and M. E. Raikh, JETP Lett. **47**, 452 (1988); T. K. Ng and P. A. Lee, Phys. Rev. Lett. **61**, 1768 (1988).
[5] L. P. Kouwenhoven, C. M. Marcus, P. L. McEuen, S. Tarucha, R. M. Westervelt, and N. S. Wingreen, in *Mesoscopic Electron Transport*, edited by L. L. Sohn, L. P. Kouwenhoven, and G. Schön, NATO Advanced Studies Institute, Series E: Applied Science (Kluwer, Dordrecht, 1997), Vol. 345, pp. 105–214.
[6] N. J. Craig, J. M. Taylor, E. A. Lester, C. M. Marcus, M. P. Hanson, and A. C. Gossard, Science **304**, 565 (2004).
[7] H. B. Heersche, Z. de Groot, J. A. Folk, L. P. Kouwenhoven, H. S. J. van der Zant, A. A. Houck, J. Labaziewicz, and I. L. Chuang, Phys. Rev. Lett. **96**, 017205 (2006).
[8] M. A. Ruderman and C. Kittel, Phys. Rev. **96**, 99 (1954); T. Kasuya, Prog. Theor. Phys. **16**, 45 (1956); K. Yoshida, Phys. Rev. **106**, 893 (1957).
[9] P. Simon, R. López, and Y. Oreg, Phys. Rev. Lett. **94**, 086602 (2005).
[10] M. G. Vavilov and L. I. Glazman, Phys. Rev. Lett. **94**, 086805 (2005).
[11] G. Zarand, C. H. Chung, P. Simon, and M. Vojta, Phys. Rev. Lett. **97**, 166802 (2006).
[12] C. H. Chung and W. Hofstetter, Phys. Rev. B **76**, 045329 (2007).
[13] V. Koerting, P. Wölfle, and J. Paaske, Phys. Rev. Lett. **99**, 036807 (2007).
[14] C. Jayaprakash, H. R. Krishna-murthy, and J. W. Wilkins, Phys. Rev. Lett. **47**, 737 (1981); B. A. Jones and C. M. Varma, *ibid.* **58**, 843 (1987); B. A. Jones, C. M. Varma, and J. W. Wilkins, *ibid.* **61**, 125 (1988); B. A. Jones and C. M. Varma, Phys. Rev. B **40**, 324 (1989); I. Affleck, A. W. W. Ludwig, and B. A. Jones, *ibid.* **52**, 9528 (1995).
[15] O. Sakai and Y. Shimizu, J. Phys. Soc. Jpn. **61**, 2333 (1992); O. Sakai and Y. Shimizu, *ibid.* **61**, 2348 (1992).
[16] J. Kroha, S. Kirchner, G. Sellier, P. Wlfle, D. Ehm, F. Reinert, S. Huefner, and C. Geibel, Physica E (Amsterdam) **18**, 69 (2003).
[17] P. S. Cornaglia and D. R. Grempel, Phys. Rev. B **71**, 075305 (2005).
[18] M. Vojta, R. Bulla, and W. Hofstetter, Phys. Rev. B **65**, 140405(R) (2002).
[19] W. Hofstetter and H. Schoeller, Phys. Rev. Lett. **88**, 016803 (2002).
[20] A. Kogan, G. Granger, M. A. Kastner, and D. Goldhaber-Gordon, Phys. Rev. B **67**, 113309 (2003).
[21] K. G. Wilson, Rev. Mod. Phys. **47**, 773 (1975); T. A. Costi, A. C. Hewson, and V. Zlatić, J. Phys.: Condens. Matter **6**, 2519 (1994); W. Hofstetter, Phys. Rev. Lett. **85**, 1508 (2000).
[22] M. Sindel, W. Hofstetter, J. von Delft, and M. Kindermann, Phys. Rev. Lett. **94**, 196602 (2005).
[23] L. Borda, L. Fritz, N. Andrei, and G. Zarand, Phys. Rev. B **75**, 235112 (2007).
[24] A.-P. Jauho, N. S. Wingreen, and Y. Meir, Phys. Rev. B **50**, 5528 (1994).
[25] C. Bruder and H. Schoeller, Phys. Rev. Lett. **72**, 1076 (1994).
[26] This cutoff is typically provided by the level spacing $\delta\epsilon$ of the quantum dots.
[27] R. Deblock, E. Onac, L. Gurevich, and L. P. Kouwenhoven, Science **301**, 203 (2003).
[28] P. Nordlander, M. Pustilnik, Y. Meir, N. S. Wingreen, and D. C. Langreth, Phys. Rev. Lett. **83**, 808 (1999).
[29] Y. Meir, N. S. Wingreen, and P. A. Lee, Phys. Rev. Lett. **70**, 2601 (1993).